PHYSICAL REVIEW B VOLUME 55, NUMBER 18 1 MAY 1997-II

Scaling behavior of an antiferroelectric hysteresis loop

Yong-Hae Kim and Jong-Jean Kim*
Department of Physics, Korea Advanced Institute of Science and Technology, Taejon 305-701, Korea
(Received 29 January 1997)

A double hysteresis loop of an antiferroelectric betaine phosphate-arsenate mixed crystal ($BP_{0.9}A_{0.1}$) was studied as a function of applied frequency Ω and field amplitude E_0. A scaling analysis of the antiferroelectric hysteresis loop was given to show $A_H \propto (E_0 - E_c)^{0.50}\Omega^{0.40}$, where A_H represents the area of the hysteresis loops and E_c a threshold field for observing the hysteresis curves. The scaling exponents are found to be close to the reported theoretical results of the two-dimensional ferromagnetic Ising models. We have also found a different scaling behavior for the antiferroelectric minor loops as $A_m \propto (E_0 - E_c)^{2.12}\Omega^{0.28}$, where A_m represents the area of the minor loops. [S0163-1829(97)51518-9]

Nonequilibrium phenomena have become a great concern of recent theoretical works in statistical mechanics and have been drawing renewed interest from many people in the renormalization-group theories of phase transition and field theories.[1–3] Nonequilibrium systems of recent scaling studies may be classified into two groups: a driven or steady state nonequilibrium system and a quenched system far from equilibrium.[3–5] For example, scaling studies of the roughness fluctuations in time and space for random deposition of particles onto a substrate surface belong to the first category while scaling studies of the time-dependent domain growth after initial nucleation and spinodal decomposition, as for a system quenched from a high-temperature disordered phase toward a low-temperature ordered phase, belong to the second category. Hysteresis loop measurements belonging to the second category but also with driven characteristics have been studied more recently.[6–12] In the soft magnet system the Steinmetz law about the relation between the area A of the hysteresis loop and the sine wave amplitude H_0 of the applied magnetic field as $A \propto H_0^{1.6}$ has long been known.[13] However, an intensive study of the hysteresis curve dependence on field amplitude and frequency was reported only recently by Rao *et al.*,[6] who applied the first-order phase transition analysis of Mazenko and Zannetti[1] to the hysteresis curve for the three-dimensional continuous $(\Phi^2)^2$ N-vector model system ($N \to \infty$). Their numerical simulation results could show a scaling behavior of the hysteresis loop area A with respect to the field amplitude H_0 and frequency Ω as

$$A \propto H_0^{\alpha}\Omega^{\beta}$$

with $\alpha = 0.66$ and $\beta = 0.33$. Hysteresis loops are characterized by saturation and distinguished from the minor loops without saturation appearing at small field amplitude. Dhar and Thomas[7] also studied the same model system but obtained $\alpha = 0.5$ and $\beta = 0.5$ for all dimensions of $d > 2$. Lo and Pelcovits[8] made a Monte Carlo simulation study of the hysteresis curve for a two-dimensional (2D) Ising model and obtained the scaling exponents of $\alpha = 0.46$ and $\beta = 0.36$. Sengupta *et al.*[9] obtained $\alpha = 0.47$ and $\beta = 0.40$ for the same 2D Ising model from the cell dynamics simulation study. He and Wang[10] applied a surface magneto-optic Kerr effect to study the hysteresis curves of Fe/Au[001] film to obtain $\alpha = 0.59$ and $\beta = 0.31$. Zhong *et al.*,[11] and Zhong and Zhang[12] also reported the hysteresis loop scaling by one single variable of the field sweeping rate.

Hysteresis loops of the ferroelectrics are drawing great interest from many people due to the recent developments of the ferroelectric thin-film applications.[14] Ferroelectric hysteresis loops were studied for their frequency and field amplitude dependence[15,16] on the basis of the Avrami model[17] where the domain wall velocity was assumed to be proportional to the applied field amplitude. Orihara *et al.*[16] derived a scaling behavior of the hysteresis curve from the Avrami model. Hashimoto *et al.*[18] obtained a scaling exponent $\beta = 0.23$ for the hysteresis curves of the ferroelectric triglycine sulphate. Ferroelectric hysteresis loops of the 1D hydrogen bonded cesium dihydrogen phosphate crystals are also shown to have scaling behaviors[19] of the extended Avrami model. However, there has been no report yet on the scaling behavior studies of the antiferroelectric or antiferromagnetic hysteresis loops.

Since the discovery of antiferroelectricity in betaine phosphate (BP, $(CH_3)_3N\ CH_2COOH_3PO_4$) by Albers *et al.*[20] betaine compounds have been a great concern in ferroelectric research.[21] Betaine arsenate (BA, $(CH_3)_3NCH_2COOH_3AsO_4$) exhibits a ferroelastic transition at $T_{c1} = 411$ K and a ferroelectric transition at $T_{c2} = 119$ K.[22] Although BP and BA are not isomorphous, and the respective hydrogen-bonded chain axes have a considerable lattice mismatch ($b = 7.852$ Å for BP and $c = 8.128$ Å for BA), mixed single crystals, $BP_{1-x}A_x$, can be grown for almost the whole range of arsenate concentration x.[23,24] Maeda and Suzuki[24] performed dielectric measurements on $BP_{1-x}A_x$ mixed crystals to obtain a full range phase diagram, where the antiferroelectric phase was found to be stable at low temperature for $0 \leqslant x \leqslant 0.4$.

Antiferroelectric double hysteresis loops are best observed in the antiferroelectric $BP_{0.9}A_{0.1}$ mixed crystal,[25] and we want to report on the scaling behavior analysis of the observed antiferroelectric hysteresis loops.

Polarization–electric field (P-E) hysteresis loops were measured by use of a programmable digital oscilloscope (LeCroy 9420). A sine wave from the function generator (HP3310A) was amplified by a home-made power amplifier

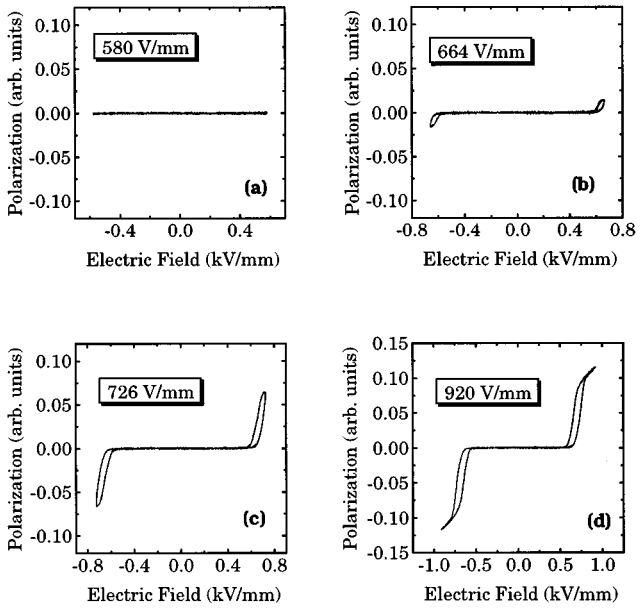

FIG. 1. Double hysteresis loops observed in the antiferroelectric $BP_{0.9}A_{0.1}$ crystal with the sine wave field of frequency $\Omega=35$ Hz and various amplitudes of (a) 580 V/mm, (b) 664 V/mm, (c) 726 V/mm, and (d) 920 V/mm.

($\times 100$) and applied to the sample capacitor. The response signal of the crystal was fed to the digital oscilloscope through an operational amplifier (LF356) for data acquisition and processing, where the linear background was automatically subtracted as in the standard Sawyer-Tower circuit. Each hysteresis curve presented was obtained after averaging over 200 samplings to average out the noise deformations. All the experimental observations of hysteresis curves are obtained in the antiferroelectric phase of $BP_{0.9}A_{0.1}$ at 79.05 K.

In Figs. 1(a)–1(d) we presented the typical hysteresis curves obtained at various field amplitudes of the sine wave input at $\Omega=35$ Hz. We can observe three different cases, where no polarization curve can be observed below a threshold field strength E_c, minor hysteresis loops without saturation at relatively small fields above E_c, and the saturated double hysteresis curves at large fields well above E_c. This sequence of field-dependent changes can be observed also at other frequencies. In Fig. 2 we have plotted the area of the hysteresis curves as a function of the applied field amplitude observed at various input frequencies from $\Omega=35$ Hz to 1 kHz. It can be seen that the field-dependent change of the area is rapid ($\alpha>1$) for minor loops but slow ($\alpha<1$) for saturated hysteresis curves. We can also observe that the range of field strength generating minor loops decreases with increasing frequency. This can be associated with the scaling behavior of the loop area in a two-component scaling variable of the form $(E_0-E_c)^{\alpha}\Omega^{\beta}$, where for a given value of the scaling variable the field component decreases with increasing frequency component. In Fig. 2 we can see the hysteresis loop observed at $E_0=900$ V/mm hardly changes in the loop area with frequency change from 300 Hz to 1 kHz, corresponding to the type-*B* region of He and Wang.[10] Scaling is restricted to the type-*A* region where the loop area

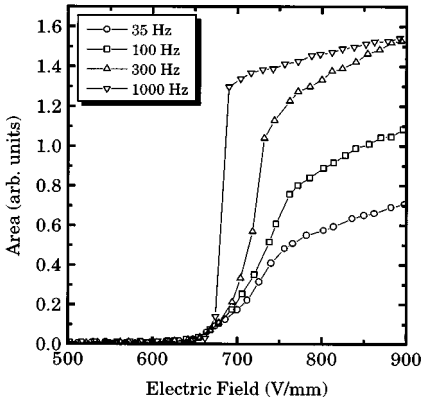

FIG. 2. The hysteresis loop area dependence on the field amplitude as observed at various frequencies from $\Omega=35$ Hz to $\Omega=1$ kHz.

increases with frequency,[6,10] and our scaling analysis is restricted to the hysteresis loops observed in the frequency region below 200 Hz.

In Fig. 3 a log-log plot is presented between the area of the hysteresis loop and frequency at a fixed field strength of 700 V/mm. We can obtain the scaling exponent β_m for minor loops as $\beta_m=0.28\pm0.03$ by fitting the frequency region below 200 Hz. In Fig. 4 we presented a log-log plot between the loop area and frequency for the hysteresis loops observed at a larger field strength of 906 V/mm. Figure 2 also shows that the saturated hysteresis loops are observed even at $\Omega=35$ Hz for the large field amplitude of 906 V/mm. We thus obtain from Fig. 4 the scaling exponent β_H for the saturated hysteresis loops as $\beta_H=0.40\pm0.04$ by fitting the type-*A* region below 200 Hz. Our experimental value of $\beta_H=0.40\pm0.04$ is in best agreement with the Ising model exponent[9] but different from the value of the ferroelectric hysteresis curve.[18]

In Fig. 5 we have shown the field strength dependence of the loop area for the hysteresis loops observed at various frequencies. In Fig. 6 we have shown the scaling fit of the minor loops of Fig. 5 with respect to the field strength as $\tilde{A}_m \propto (E_0-E_c)^{\alpha_m}$, where $\tilde{A}_m$ signifies the frequency scaled

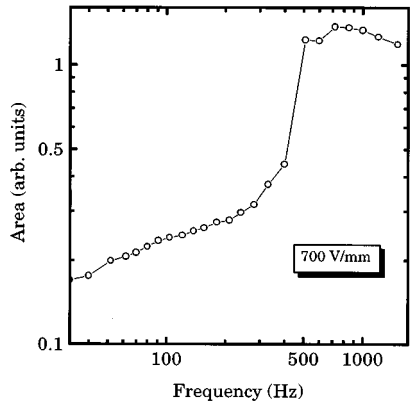

FIG. 3. Log-log plot between the hysteresis loop area and the applied frequency Ω of the field with the field amplitude fixed at $E_0=700$ V/mm. From the data fit we obtain $\beta_m=0.28\pm0.03$ for $\Omega\leqslant 200$ Hz.

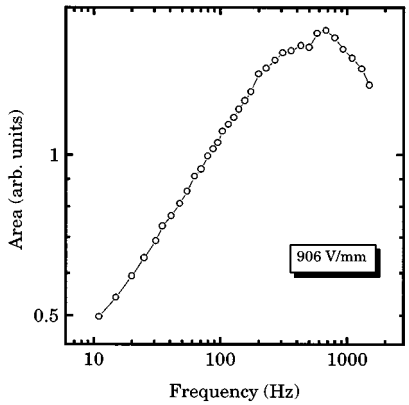

FIG. 4. Log-log plot between the hysteresis loop area and the applied frequency Ω of the field with the field amplitude fixed at $E_0=906$ V/mm. From the data fit we obtain $\beta_H=0.40\pm0.04$ for $\Omega\leqslant200$ Hz.

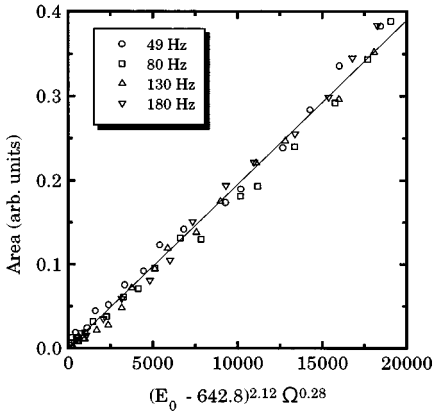

FIG. 6. Scaling plot of the minor loop area (A_m) dependence on field amplitude (E_0) and frequency (Ω) using the data set of Fig. 5: $A_m\propto(E_0-E_c)^{\alpha_m}\Omega^{\beta_m}$ with $\alpha_m=2.12\pm0.02$, $\beta_m=0.28\pm0.03$, and $E_c=642.8$ V/mm.

area of minor loop by using β_m obtained from Fig. 3. In antiferroelectrics we cannot observe the hysteresis loops unless we increase the field strength above a threshold value and we must express the effective field strength as (E_0-E_c) in contrast to the ferroelectrics. We have obtained from fitting $\alpha_m=2.12\pm0.02$ and $E_c=642.8$ V/mm. In Fig. 7 we have shown a similar scaling fit for the saturated hysteresis loops of Fig. 5 with respect to the field strength as $\widetilde{A}_H\propto(E_0-E_c)^{\alpha_H}$, where $\widetilde{A}_H$ signifies the frequency scaled area of hysteresis loop by using β_H obtained from Fig. 4, and $E_c=642.8$ V/mm. The scaling exponent α_H was obtained from the fit as $\alpha_H=0.50\pm0.02$, which is in reasonable agreement with the Ising model values[8,9] but in considerable difference from the values of Rao *et al.*[6] and the thin-film experiment.[10]

It is very interesting to note the similar values of the scaling exponent between the antiferroelectric hysteresis loop of the $BP_{0.9}A_{0.1}$ crystal and the ferromagnetic hysteresis loop of the 2D Ising model. Although the equilibrium properties of the phase transition have the same critical exponents between ferromagnetic and antiferromagnetic systems,[3] it is not obvious to expect the same in the nonequilibrium properties of the two systems such as a hysteresis curve characterized by nucleation and domain growth.

In the case of ferroelectric hysteresis loops, when we apply an electric field $E=E_+>0$ the ferroelectric system of spontaneous polarization P tends to have a global minimum of energy at $P=P_+>0$ and a metastable local minimum at $P=P_-<0$. If the system were at $P_-<0$ under the external field $E_+>0$, a transition to the $P_+>0$ state of the global minimum energy may be induced from the nucleation fluctuation and the succeeding domain growth.[26] Meanwhile in the antiferroelectric system we have two minimum energy wells at P_{+-} and P_{-+} which remain to be equivalent under the external uniform electric field. When we apply an electric field $E=E_+>0$ larger than a threshold field E_c the sublattice polarization with $P_-<0$ will become metastable against the $P_+>0$ state, that is, under a strong electric field $E_+>E_c$ the antiferroelectric polarization P_{+-} or P_{-+} becomes metastable against the ferroelectric polarization $P_{++}>0$. Field-induced local polarizations in the metastable state would tend to nucleation and subsequent domain growth, leading to the ferroelectric polarization P_{++}.

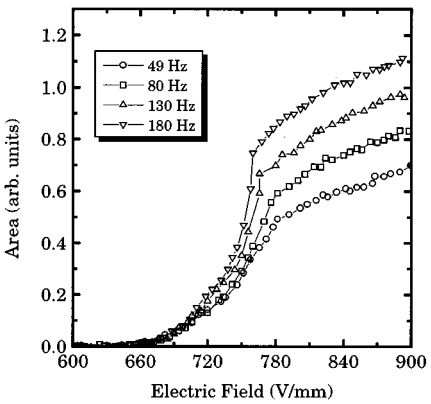

FIG. 5. Applied field amplitude and frequency dependence of the hysteresis loop area in the region appropriate for scaling analysis.

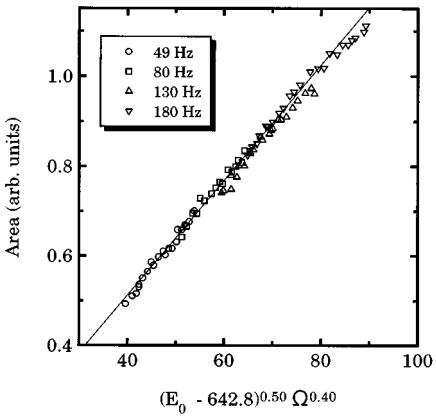

FIG. 7. Scaling plot of the saturated hysteresis loop area (A_H) dependence on field amplitude (E_0) and frequency (Ω) using the data set of Fig. 5: $A_H\propto(E_0-E_c)^{\alpha_H}\Omega^{\beta_H}$ with $\alpha_H=0.50\pm0.02$, $\beta_H=0.40\pm0.04$, and $E_c=642.8$ V/mm.

We can thus see the kinematic steps of the field-induced transitions encountered with both ferroelectric and antiferroelectric hysteresis loops are similar to each other except the threshold field effect in the antiferroelectric hysteresis loops. However, since the electrostatic energy would increase with increasing surface polarization, the ferroelectric system tends to form a more stable multidomain structure whereas in the antiferroelectrics of no surface polarization the antiferroelectric structure remains more stable against the ferroelectric structure. Thus we do not expect a spontaneous transition from the antiferroelectric minimum state to the ferroelectric minimum state at $E=E_c$. The field-induced ferroelectric state at $E=E_c$, however, would tend to transform to the antiferroelectric state of the double minimum well with decreasing field below E_c. In other words, due to this difference in electrostatic surface energy between the ferroelectric and antiferroelectric state, kinematic symmetry of the hysteresis loop formation is conserved in the ferroelectric hysteresis loop with respect to $E=0$ but broken in the antiferroelectric hysteresis loop with respect to $E=E_c$.

In conclusion we have observed in the antiferroelectric system of the $BP_{1-x}A_x$ ($x=0.1$) crystal a scaling behavior of the hysteresis curve as $A\propto(E_0-E_c)^{\alpha}\Omega^{\beta}$, where we have found $\alpha_m=2.21\pm0.02$, $\beta_m=0.28\pm0.03$ for the unsaturated minor loops, and $\alpha_H=0.50\pm0.02$, $\beta_H=0.40\pm0.04$ for the saturated hysteresis loops. The scaling exponents α_H and β_H are found to be close to the reported theoretical values of the two-dimensional ferromagnetic Ising models. This observation is reminiscent of the equilibrium phase transition where both ferromagnetic and antiferromagnetic Ising spin systems belong to the same universality class.[3]

This work was supported in part by the Korea Science and Engineering Foundation through the RCDAMP at Pusan National University.

*Author to whom correspondence should be addressed.

[1] G. F. Mazenko and M. Zannetti, Phys. Rev. B **32**, 4565 (1985).
[2] For a review, see A. J. Bray, Adv. Phys. **43**, 357 (1994); R. F. Streater, *Statistical Dynamics* (Imperial College Press, London, 1995).
[3] N. Goldenfeld, *Lectures on Phase Transitions and the Renormalization Group* (Addison-Wesley, New York, 1992).
[4] *Dynamics of Fractal Surfaces*, edited by F. Family and T. Vicsek (World Scientific, Singapore, 1991).
[5] *Solids far from Equilibrium: Growth, Morphology and Defects*, edited by C. Godreche (Cambridge University Press, New York, 1991).
[6] M. Rao, H. R. Krishnamurthy, and R. Pandit, Phys. Rev. B **42**, 856 (1990); **43**, 3373 (1991).
[7] D. Dhar and P. B. Thomas, J. Phys. A **25**, 4967 (1990).
[8] W. S. Lo and R. A. Pelcovits, Phys. Rev. A **42**, 7471 (1990).
[9] S. Sengupta, Y. Marathe, and S. Puri, Phys. Rev. B **45**, 7828 (1992).
[10] Y. L. He and G. C. Wang, Phys. Rev. Lett. **70**, 2336 (1993).
[11] F. Zhong, J. X. Zhang, and G. G. Siu, J. Phys. Condens. Matter. **6**, 7785 (1994).
[12] F. Zhong and J. X. Zhang, Phys. Rev. Lett. **75**, 2027 (1995).
[13] C. P. Steinmetz, Trans. Am. Inst. Elec. Eng. **9**, 3 (1892).
[14] J. F. Scott and C. A. Araujo, Science **246**, 1400 (1989).
[15] J. Hataro, J. Phys. Soc. Jpn. **45**, 1291 (1978).
[16] H. Orihara, S. Hashimoto, and Y. Ishibashi, J. Phys. Soc. Jpn. **63**, 1031 (1994).
[17] M. Avrami, J. Chem. Phys. **7**, 1103 (1939); **8**, 212 (1940); **9**, 177 (1941).
[18] S. Hashimoto, H. Orihara, and Y. Ishibashi, J. Phys. Soc. Jpn. **63**, 1610 (1994).
[19] J.-G. You and J.-J. Kim, J. Phys. Soc. Jpn. **65**, 3362 (1996).
[20] J. Albers, A. Klöpperpieper, A. J. Rother, and K. H. Ehses, Phys. Status Solidi A **74**, 553 (1982).
[21] J. Albers, Ferroelectrics **78**, 3 (1988).
[22] K. Klöpperpieper, H. J. Rother, J. Albers, and K. H. Ehses, Ferroelectr. Lett. Sect. **44**, 115 (1982).
[23] M. Maeda, Ferroelectrics **96**, 269 (1989).
[24] M. Maeda and I. Suzuki, Ferroelectrics **108**, 351 (1990).
[25] Y.-H. Kim, B.-G. Kim, J.-J. Kim, T. Mochida, and S. Miyajima, J. Phys. Condens. Matter. **8**, 6095 (1996).
[26] R. Landauer, D. R. Young, and M. E. Drougard, J. Appl. Phys. **27**, 752 (1956).